Original Research Article: full paper

(2023), «EUREKA: Physics and Engineering»
Number 2

DEVELOPMENT OF MESOPOROUS ACTIVATED CARBONS DERIVED FROM BREWED COFFEE WASTE FOR CO_2 ADSORPTION

Dewa Ngakan Ketut Putra Negara✉
Department of Mechanical Engineering[1]
devputranegara@unud.ac.id

I Made Widiyarta
Department of Mechanical Engineering[1]

I Gusti Agung Kade Suriadi
Department of Industrial Engineering[1]

I Gusti Komang Dwijana
Department of Mechanical Engineering[1]

I Made Dwi Budiana Penindra
Department of Industrial Engineering[1]

I Gusti Ngurah Putu Tenaya
Department of Mechanical Engineering[1]

I Gusti Ketut Sukadana
Department of Mechanical Engineering[1]

Anton Saladin Ferdinand
Department of Mechanical Engineering[1]

[1]*Udayana University*
Jl. Raya Kampus Unud, Jimbaran, Badung, Bali, Indonesia, 80361

✉**Corresponding author**

Abstract

The primary cause of rising CO_2 concentrations in the atmosphere is the use of fossil fuels in motor vehicles and factory activities in industry. CO_2 levels in the atmosphere can be controlled and reduced by using low-carbon energy and capturing and storing CO_2. One widely used way for CO_2 capture and storage is adsorption method. This method necessitates the use of an adsorbent, one of which is activated carbon. In this study, brewed coffee waste was converted into activated carbons, characterized, and tested for carbon dioxide adsorption. Brewed coffee waste was dehydrated at 105 °C for an hour before being carbonized at 550 °C and activated at 670, 700, and 730 °C, with a 200-ml/min nitrogen injection during activation. Activated carbons with activation temperatures of 670, 700, and 730 °C were denoted as AC-670, AC-700, and AC-730, respectively. A series of TGA, SEM, and adsorption isotherm tests were used to determine the proximate components, surface morphology, and surface structure of the activated carbons produced. To assess the adsorption capacities of activated carbon on CO_2, the gravimetric CO_2 adsorption isotherm method was used. According to the findings of the study, increasing activation temperatures cause variable properties in activated carbon. When using an activation temperature of 700 °C, the most appropriate properties of activated carbon can be obtained. It has 425.843 m^2/g specific surface area, 0.345 cm^3/g pore volume, 3.423 nm pore diameter, 235.628 cm^3/g nitrogen adsorption capacity, and 4.183 mmol/g CO_2 adsorption performance. This study provided a simple way converting brewed coffee waste into activated carbon with excellent performance for CO_2 adsorption.

Keywords: activated carbon, adsorption, CO_2, coffee, activation, mesoporous, carbonization, nitrogen, surface area, pore diameter.

DOI: 10.21303/2461-4262.2023.002809

1. Introduction

The increase in human activity and productivity in the industrial sector is one of the reasons for the increasing concentration of carbon dioxide (CO_2) in the atmosphere [1]. Even now, the concentration has surpassed 412 mole fraction (ppm) [2], and it is predicted to rise further in the

coming year. The use of fossil fuels is a major contributor to the CO_2 content of the atmosphere [3]. This is due to the fact that, until recently, fossil fuels were the primary source of energy [4]. Excess CO_2 in the atmosphere can cause the greenhouse effect, rising sea levels, extreme weather, and global warming [1], all of which are serious environmental issues that, in the long term, threaten life on Earth. This is a serious problem that has received attention from the international community, and various efforts must be made to control and reduce CO_2 concentrations in the atmosphere. Controlling and reducing CO_2 emissions from industry can be accomplished through two methods [1]; increasing the use of low-carbon energy [5] and capturing and storing CO_2 [4]. Carbon dioxide capture and storage is widely regarded as the most important technology for lowering CO_2 emissions in the atmosphere [6]. Adsorption of CO_2 using an adsorbent is one of the most effective methods because of its low energy consumption and wide application [7]. Materials that have been used as adsorbents include: activated carbon [8, 9], zeolite [10], and metal-organic frameworks [11]. Activated carbon is the most effective and widely used adsorbent [12] due to its wide availability, high thermal stability, low cost [13], and its pore structure with a large pore volume and a high specific surface area.

As a carbon-based substance known as activated carbon, it possesses a complex pore structure, a huge pore surface area, the ability to chemically alter its surface, and a variety of methods for modifying the porous structure [14]. Activated carbon is often made from a variety of raw materials that have a high carbon content and a low inorganic content and is commonly manufactured by dehydration, carbonization, and activation steps. In order to reduce the cost of producing activated carbon, the manufacturing process' efficiency must be improved by using less expensive raw materials and activating processes at lower temperatures. Biomass is a plentiful and reasonably priced source of raw materials [15], which includes bamboo [16, 17], sawdust [18–20], agricultural waste [21], rice husk [22], and others. Coffee is one of the most prevalent biomasses and is the second largest commodity in world trade [23]. The large commodity of coffee produces a significant byproduct in the form of coffee waste. Chemically converting coffee waste into activated carbon with variations in the impregnation ratio, has been researched, and is used for a variety of purposes. Activated carbon produced using KOH activating agent with impregnation ratios (IR) char/KOH 1:0, 2:1, 1:1, and 2:3 was used to adsorb caffeine [24]; activated carbon-KOH activation with an IR of 9:1 was applied for capacitive deionization [25]; and activated carbon-H_3PO_4 activation with an IR of 50 and 100 % wt. was used for organic matter removal from landfill leachate [26]. However, finding coffee waste-activated carbon that has been physically activated and used to absorb CO_2 is difficult. Although physical activation is simpler than chemical activation and does not involve chemicals that could lead to new sources of pollution, the reason why it is not used in the journals surveyed is not explicitly stated. As a result, researching the use of physical activation in the production of activated carbon from coffee waste and its application to CO_2 adsorption is extremely important.

The goal of this study is to propose a low-cost and efficient method for physically converting brewed coffee waste into activated carbon at various activation temperatures by employing *N*-doping as an activating agent. It was investigated how activation temperatures affect activated carbon properties such as proximate composition, morphology, and surface texture. Furthermore, the activated carbons were used for CO_2 adsorption and their performance was compared to that of some chemically activated carbons.

2. Materials and methods

2. 1. Preparation of Activated Carbons

Brewed coffee waste was collected from a small coffee shop in Denpasar City, Bali, Indonesia. The material was dehydrated for an hour in a programmable electric furnace set at 105 °C before being cooled to room temperature. The dehydrated sample was then carbonized by raising its temperature to 550 °C in an oxygen-free environment, holding it for 25 minutes, and then allowing it to cool in the furnace for 12 hours. After that, a 60-mesh was used to weave the carbonized sample. Three temperature activations were used: 670, 700, and 730 °C with a 25-minute and 12-hour holding and cooling periods, respectively. A 200 ml/min nitrogen was injected during activation into

the reactor housing the sample. The activated carbons yielded were designated as AC-670, AC-700, and AC-730, respectively, for the temperatures at which they activated.

2. 2. Characterization of Activated Carbons

A series of characterizations, including proximate, SEM, and adsorption isotherm tests, were performed to determine the proximate composition, surface morphology, and surface texture of activated carbon, respectively. The thermogravimetric analyzer, TGA 701 device (ASTM D7582 MVA Biomass), SEM-JSM-651OLA, and Quantachrome Nova Instruments Version 11.0 were used for proximate, surface morphology, and surface texture characterization, respectively. The surface texture of activated carbons includes BET surface area (S_{BET}), pore volume (V_P), and average pore diameter (D_P). S_{BET} was determined at relative pressures of 0.099–0.296, 0.097–0.304, and 0.1–0.296 for AC-670, AC-700, and AC-730, respectively, using BET (Brunaeur-Emmet-Teller) analysis.

2. 3. CO_2 Adsorption Isotherm Tests

The schematic of the gravimetric CO_2 adsorption isotherm test is depicted in **Fig. 1**.

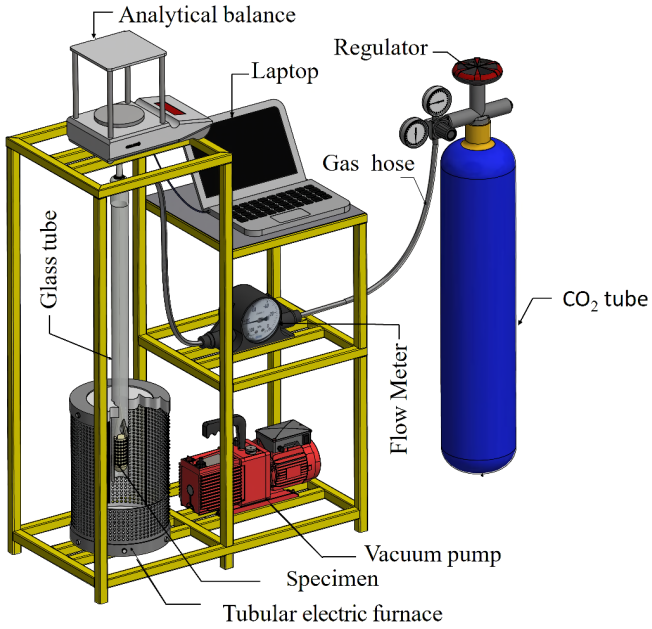

Fig. 1. Schematic of CO_2 adsorption isotherm test using gravimetric method

The weight of the chamber in which the sample is placed is recorded as m_c. The chamber is partially filled with activated carbon AC-670. The chamber is then attached to a wire that is connected to a digital balance. The glass tube is then installed so that the chamber and wire are contained within it. The glass tube's end is inserted into the vertical tubular furnace until the entire chamber is inside. To remove the remaining gases in the activated carbon, a degassing process is carried out by heating the sample to 200 °C and then vacuuming for 30 minutes. The sample was then cooled to room temperature, and the chamber, which contained activated carbon AC-670 was then weighed and recorded as m_i. Furthermore, the temperature of the tubular electric furnace was set to 30 °C, and CO_2 was injected into the sample at a constant pressure of 1 bar once the set temperature was reached. The chamber mass change is measured using a digital analytical balance and automatically recorded as an excel file on a computer. When the mass change is constant, it indicates the adsorption equilibrium has been reached and the test was completed. The adsorption process's final mass was determined and expressed as m_f. The test was repeated three times, and the same procedure was used to evaluate AC-700 and AC-730 activated carbons. The total mass of CO_2 absorbed (m_{CO_2}) is defined as the difference between m_f and m_i and can be calculated using (1).

The specific adsorption capacity (S_{CO_2}) of activated carbon was calculated using (2), where $MrCO_2$ is the relative molecule mass of CO_2 (44 g/mol), and m_{ac} is the mass of activated carbon (g) that was obtained using (3):

$$m_{CO_2} = m_f - m_i, \text{ (g)}, \tag{1}$$

$$S_{CO_2} = \frac{m_{CO_2}}{MrCO_2 \cdot m_{ac}} \cdot 1000 \left(\frac{\text{mmol}}{\text{g}} \right), \tag{2}$$

$$m_{ac} = m_i - m_c. \tag{3}$$

3. Result and discussions

3. 1. TGA analysis

Fig. 2 depicts the composition of proximate activated carbon as determined by the TGA test. The moisture, volatile, ash, and fix carbon contents of activated carbon range from 7.7–8.56 %, 13.68–16.79 %, 3.78–5.05 %, and 71.71–73.62 %, respectively. Increasing the activation temperature resulted in fluctuating compositions of moisture, volatile, and ash. The higher the activation temperature, however, the higher the fix carbon, though the increase was not significant. Except for AC-670, whose volatile content exceeds 15 %, AC-700 and AC-730 activated carbons have a proximate composition that meets the Indonesian National Standard SNI 06-3730-1995, which requires a maximum of 15 %, 25 %, and 10 % for moisture, volatile, and ash, respectively, and at least 65 % fix carbon. According to **Fig. 2**, no activated carbon outperforms the others in terms of proximate composition. A good composition of activated carbon has a high fix carbon content, low ash, moisture, and volatile content [27].

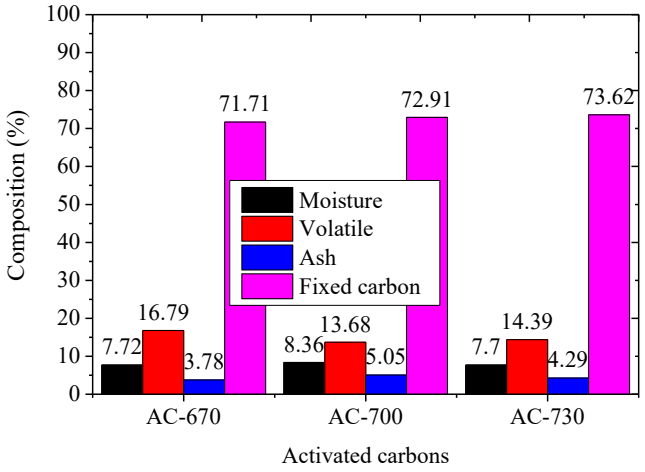

Fig. 2. Proximate components of activated carbons

3. 2. Adsorption isotherm and pore size distribution

The adsorption and desorption isotherm curve, shown in **Fig. 3**, represents the relationship between the amount of nitrogen absorbed and released by activated carbons at various relative pressure levels.

There was a significant increase in nitrogen uptake with increasing relative pressure on activated carbon, except for AC-730. As the relative pressure rises, more nitrogen molecules enter the activated carbon pore volume. Because of the low pore surface area and pore volume of AC-730, as shown in **Table 2**, its storage capacity is also limited. The lack of significant adsorption at relatively low pressures indicates that there is no filling process in microporous of activated carbon due to mostly pores of activated carbon are mesoporous and almost without microporous. This matches with the average pore diameter of activated carbons, which is mesoporous, as shown in **Table 1**. Another indication of mesoporous activated carbons is the presence of a hysteresis loop on the

adsorption-desorption isotherm curve, as shown in **Fig. 3**. The graph of the adsorption isotherms of AC-700 yields the highest adsorption at each relative pressure, indicating that adsorption by AC-700 is most effective compared to AC-670 and AC-730 due to its most appropriate surface structure characteristics, as shown in **Table 1**.

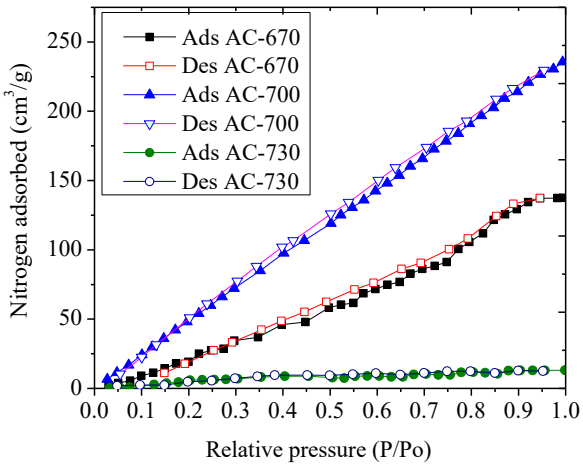

Fig. 3. Adsorption and desorption isotherm of activated carbons

The pore size distribution (PSD) of AC-670, AC-700, and AC-730 with a pore range of up to 30 nm and 6 nm in the inset image is shown in **Fig. 4**. The PSD graph depicts the relationship between the nitrogen specific adsorption capacity of activated carbon at various pore sizes. The pores of AC-670 are bimodally distributed, with two peaks located in the mesoporous region at around pore diameters of 3.5 nm and 6.5 nm, with an adsorption capacity of 0.05 $cm^3/g/nm$ and 0.02 $cm^3/g/nm$, respectively. AC-700 has a single peak (0.068 $cm^3/g/nm$) at a pore diameter of 3 nm and is monomodally distributed. Meanwhile, AC-730 has three peaks that are distributed throughout the mesoporous region (2–50 nm), with the highest peak (0.014 $cm^3/g/nm$) obtained at a pore diameter of 2.5 nm.

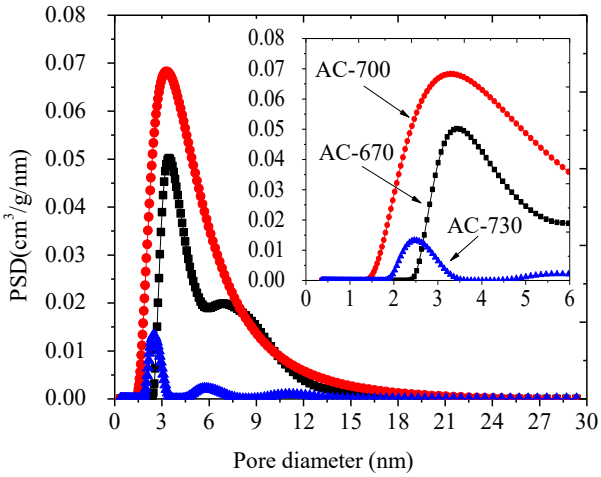

Fig. 4. Pore size distribution (PSD) of activated carbons with pore size until 30 nm and was set until 6 nm (inzet)

Fig. 5 illustrates the PSD and cumulative PSD of activated carbon. The cumulative amount of nitrogen absorbed in the pore size distribution of activated carbon is referred to as PSD cumulative. The cumulative PSD of activated carbon is the same with the pore volume of activated carbon, as shown in **Fig. 5** and **Table 1**. As the activation temperature rises, the pore volume fluctuates, with AC-670, AC-700, and AC-730 having pore volumes of 0.212, 0.345, and 0.017 cm^3/g, respectively.

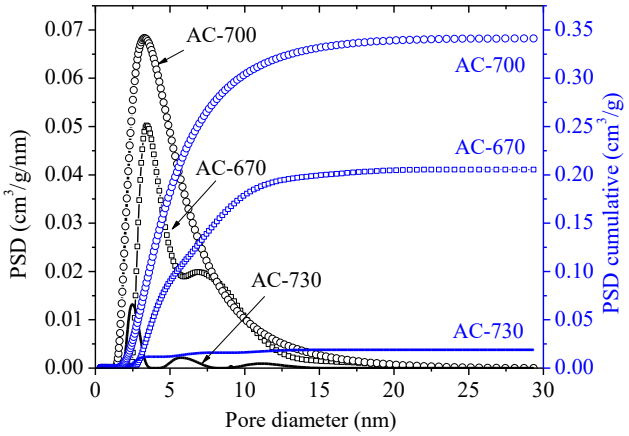

Fig. 5. PSD and PSD cumulative of activated carbons

3. 3. Surface structure and morphology of activated carbon

Table 1 shows the surface structure of activated carbons including the specific surface area (S_{BET}), specific pore volume(V_P), and average pore diameter (D_P). Activated carbon's S_{BET}, V_P, and D_P values ranged from 67.798 to 425.843 m^3/g, cm^3/g, and 2.006–3.423 nm, respectively. Increasing the activation temperature from 670 to 700 °C increased the S_{BET} by 21.50 %, the V_P by 62.73 %, and the nitrogen adsorption by 71.38 %. The S_{BET}, V_P, and nitrogen adsorption capacity decreased by 84.07 %, 95.07 %, and 94.43 %, respectively, when the temperature was raised from 700 to 730 °C. S_{BET} increases proportionally to the amount of V_P and nitrogen adsorbed.

Table 1
Surface structure of activated carbons

Sample	Surface Structure			N_2 adsorbed
	S_{BET} (m^2/g)	V_P (cm^3/g)	D_P (nm)	(cm^3/g)
AC-670	350.491	0.212	2.422	137.487
AC-700	425.843	0.345	3.423	235.628
AC-730	67.796	0.017	2.006	13.105

Several researchers used coffee waste precursors to investigate the surface structure of activated carbon. It was reported that activated carbon from coffee grounds activated using chemical activation (KOH) with a 9:1 impregnation ratio produced a surface pore area of 323.167 m^2/g, a pore volume of 0.2607 cm^3/g, an average pore diameter of 3.716 nm, and nitrogen adsorption capacity of 145 cm^3/g [25]. Activated carbon from ground coffee waste produced a pore surface area of 23.3–579.9 m^2/g, a pore volume of 0.068–0.365 cm^3/g, and an average pore diameter of 2.4–5.6 nm after a series process of carbonization at 600 °C and activation at 650 and 700 °C with an activating agent CO_2 [28]. Activated carbon from ground coffee was also chemically produced using H_3PO_4 in 50 and 100 % ratios, pyrolysis temperatures of 350 and 500 °C, and produced an average pore surface area, pore volume, and pore diameter of about 188–2118 m^2/g, 0.030–0.182 cm^3/g, and 2.5–34 nm, respectively [26]. According to the journals surveyed, activated carbon made from ground coffee produces an average pore diameter in the mesoporous range (2–50 nm), and including result obtained in this research.

Fig. 6 shows the surface morphology of activated carbons AC-670, AC-700, and AC-730 at 5000x magnification. The surface morphology of three activated carbons is distinguished by heterogeneity, irregular pore shapes, and the distribution of cavitation. The carbonization and activation processes resulted in the formation of these pores. The surface morphology is hard to differentiate from the SEM image in this study. The surface structures of activated carbons, however, have been resolved using an adsorption isotherm test, as shown in **Table 1**.

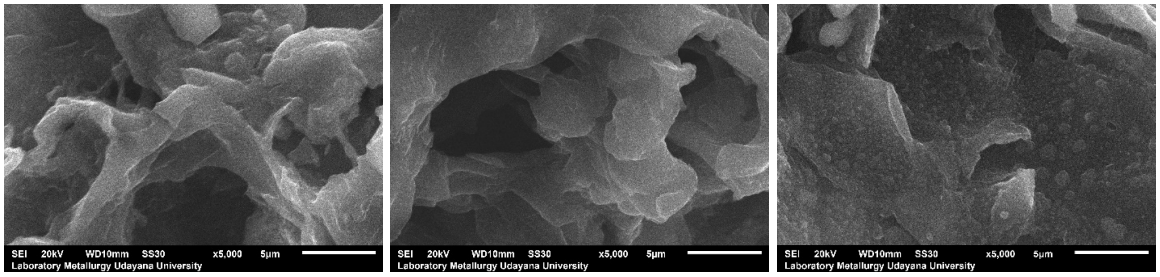

a *b* *c*

Fig. 6. Surface morphology of activated carbons at 5000x magnification:
a – AC-670; *b* – AC-700; *c* – AC-730

3. 4. Adsorption of CO_2

The CO_2 adsorption capacities of activated carbons is displayed in **Table 2**. As is the case with surface structure and nitrogen uptake, increasing the activation temperature also results in fluctuating CO_2 adsorption capacity. Increasing the activation temperature from 670 to 700 °C resulted in an average increase of 28.05 % in CO_2 adsorption. The adsorption capacity decreased by 33.64 %, from 4.1833 mmol/g to 2.7758 mmol/g when the temperature was raised from 700 to 730 °C. The CO_2 adsorption capacity of activated carbon is closely related to its pore structure and pore size distribution. When compared to AC-670 and AC-730, activated carbon AC-700 has the highest CO_2 adsorption capacity due to its larger pore surface area, and larger pore volume.

Table 2
CO_2 adsorption on the activated carbons

Samples	Initial mass	Final mass	Adsorbed mass	
	m_i (g)	m_f (g)	m_{CO_2} (g)	S_{CO_2} (mmol/g)
AC-670	1.5696	1.6334	0.0638	2.9000
	1.5710	1.6415	0.0705	3.2045
	1.5923	1.6736	0.0813	3.6955
Average	1.5776	1.6495	0.0719	3.2667
AC-700	1.7493	1.8461	0.0968	4.4000
	1.7106	1.7968	0.0862	3.9182
	1.7367	1.8298	0.0931	4.2318
Average	1.7322	1.8242	0.0920	4.1833
AC-730	1.7202	1.7897	0.0695	3.1591
	1.7165	1.7672	0.0507	2.3045
	1.7312	1.7942	0.0630	2.8636
Average	1.7226	1.7837	0.0611	2.7758

There have been numerous studies on CO_2 adsorption on various adsorbents, some of which are listed in **Table 3**. The waste-activated carbon from brewed coffee, particularly AC-700, has a higher CO_2 adsorption capacity than most other adsorbents but is still inferior to sugarcane bagasse-activated carbon with KOH activation and Brazil nut shell-activated carbon with N-doping KOH activation. Thus, brewed coffee waste is a promising alternative raw material for the production of activated carbon because it can only be physically activated using nitrogen to yield activated carbon with a CO_2 adsorption rate comparable to other chemically activated adsorbents. In addition, by not requiring chemicals in its manufacturing process, it can reduce costs while producing no new waste.

Table 3
The comparison of CO_2 adsorption performance

Materials/activated carbons	CO_2 adsorption (mmol/g)
Sugarcane bagasse activated carbon, KOH activation [1]	1.66–4.8
Rice husks activated carbon, CO_2 activation, and washed with K_2CO_3 [22]	0.5–3.5
Olive pomace activated carbon, K_2CO_3 impregnation, N-doping [29]	0.79–3.15
Microalgae/poplar sawdust activated carbon, N-doping [30]	2.38–4.14
Bamboo activated carbon, KOH activation [31]	1.25–3.25
Waste walnut shell activated carbon, N-doped, KOH, K_2CO_3 and ZnCl activator [32]	0.38–5.13
PAN-based activated carbon [33]	0.3–1.2
Potassium bitartrate-derived porous carbons (at 25 °C) [34]	2.68–3.55
Brazil nut shells-activated carbon, KOH-activation and N-doping using melamine [14]	4.16–5.30
Biomass chitosan and graphitic carbon nitride, N-doping [35]	2.94–3.91
Maize Cob Waste-Activated carbon, CO_2 activation (MCW (PA)3 h) [36]	1.62–1.71
Olive pomace-activated carbon, steam-K_2CO_3 activation [29]	1.72–3.15
N-doped hierarchically ordered micro-mesoporous carbons (NHOMCs) [12]	2.17–4.02
Face masks-activated carbon, KOH activation, 800 °C [37]	3.9
Brewed coffee waste-activated carbon, N-doping **[this study]**	2.77–4.18

3. 5. Limitations of the research and directions of its development

This investigation is still ongoing in the laboratory. More study is required before they may be used in practical settings, such as to adsorb CO_2 from factories or motorized vehicles. Future research on activated carbon is likely to focus on issues related to the design of activated carbon storage containers and determining how to regenerate activated carbon in an inexpensive and simple manner.

4. Conclusions

Brewed coffee waste has been successfully converted into activated carbons with nitrogen doping at various activation temperatures, capable of producing a surface area of 67.794–423.843 m^2/g, a pore volume of 0.017–0.345 cm^3/g, and an average pore diameter of 2.06–3.423 nm. Activation at 700 °C (AC-700) resulted in a combination of micro-and mesoporous structures, dominated by mesoporous structures. With an average pore diameter of 3.423 nm, an S_{BET} value of 425.843 m^2/g, and a pore volume of 0.345 cm^3/g, AC-700 produces high adsorption of CO_2. At a pressure of 1 bar and a temperature of 30 °C, this activated carbon has a specific adsorption capacity of 4.18 mmol/g. Thus, the application of physical activation with a nitrogen-activating agent at a temperature of 700 °C produces brewed coffee waste-activated carbon with optimal characteristics and high performance for CO_2 adsorption. However, this research is still in laboratory scale and in the future research needs to find out the way to apply in real condition.

Conflict of interest

The authors declare that they have no conflict of interest in relation to this research, whether financial, personal, authorship or otherwise, that could affect the research and its results presented in this paper.

Financing

This research is found by Udayana University's Research and Community Service Institute (LPPM) through the Udayana Flagship Research Scheme with contract number: B/78.145/UN14.4.A/PT.01.03/2022, fiscal year 2022.

Data availability

Data will be made available on reasonable request.

Acknowledgments

The authors would like to thank Udayana University's Research and Community Service Institute (LPPM), Mechanical Engineering Department, and Faculty of Engineering Udayana University for their assistance with this research.

References

[1] Han, J., Zhang, L., Zhao, B., Qin, L., Wang, Y., Xing, F. (2019). The N-doped activated carbon derived from sugarcane bagasse for CO_2 adsorption. Industrial Crops and Products, 128, 290–297. doi: https://doi.org/10.1016/j.indcrop.2018.11.028

[2] Trends in atmospheric carbon dioxide. Global Monitoring Laboratory. Earth System Research Laboratories. Available at: https://gml.noaa.gov/ccgg/trends/

[3] Ma, X., Wu, Y., Fang, M., Liu, B., Chen, R., Shi, R. et al. (2022). In-situ activated ultramicroporous carbon materials derived from waste biomass for CO_2 capture and benzene adsorption. Biomass and Bioenergy, 158, 106353. doi: https://doi.org/10.1016/j.biombioe.2022.106353

[4] Manyà, J. J., González, B., Azuara, M., Arner, G. (2018). Ultra-microporous adsorbents prepared from vine shoots-derived biochar with high CO_2 uptake and CO_2/N_2 selectivity. Chemical Engineering Journal, 345, 631–639. doi: https://doi.org/10.1016/j.cej.2018.01.092

[5] Han, J., Liang, Y., Hu, J., Qin, L., Street, J., Lu, Y., Yu, F. (2017). Modeling downdraft biomass gasification process by restricting chemical reaction equilibrium with Aspen Plus. Energy Conversion and Management, 153, 641–648. doi: https://doi.org/10.1016/j.enconman.2017.10.030

[6] Wan Zainal, W. N. H., Tan, S. H., Ahmad, M. A. (2019). Controlled Carbonization Heating Rate for Enhancing CO_2 Separation Based on Single Gas Studies. Periodica Polytechnica Chemical Engineering, 65 (1), 97–104. doi: https://doi.org/10.3311/ppch.14397

[7] Rao, N., Wang, M., Shang, Z., Hou, Y., Fan, G., Li, J. (2018). CO_2 Adsorption by Amine-Functionalized MCM-41: A Comparison between Impregnation and Grafting Modification Methods. Energy & Fuels, 32 (1), 670–677. doi: https://doi.org/10.1021/acs.energyfuels.7b02906

[8] Danish, M., Ahmad, T., Majeed, S., Ahmad, M., Ziyang, L., Pin, Z., Shakeel Iqubal, S. M. (2018). Use of banana trunk waste as activated carbon in scavenging methylene blue dye: Kinetic, thermodynamic, and isotherm studies. Bioresource Technology Reports, 3, 127–137. doi: https://doi.org/10.1016/j.biteb.2018.07.007

[9] Negara, D. N. K. P., Nindhia, T. G. T., Sucipta, M., Surata, I. W., Astrawan, K. S., Wangsa, I. P. H. (2021). Simultaneous adsorption of motorcycle emissions through bamboo-activated carbon. International Journal of Global Energy Issues, 43 (2/3), 199. doi: https://doi.org/10.1504/ijgei.2021.115144

[10] Bacariza, M. C., Graça, I., Bebiano, S. S., Lopes, J. M., Henriques, C. (2018). Micro- and mesoporous supports for CO_2 methanation catalysts: A comparison between SBA-15, MCM-41 and USY zeolite. Chemical Engineering Science, 175, 72–83. doi: https://doi.org/10.1016/j.ces.2017.09.027

[11] Qasem, N. A. A., Ben-Mansour, R., Habib, M. A. (2018). An efficient CO_2 adsorptive storage using MOF-5 and MOF-177. Applied Energy, 210, 317–326. doi: https://doi.org/10.1016/j.apenergy.2017.11.011

[12] Nasrullah, A., Bhat, A. H., Naeem, A., Isa, M. H., Danish, M. (2018). High surface area mesoporous activated carbon-alginate beads for efficient removal of methylene blue. International Journal of Biological Macromolecules, 107, 1792–1799. doi: https://doi.org/10.1016/j.ijbiomac.2017.10.045

[13] Shi, J., Cui, H., Xu, J., Yan, N., You, S. (2022). Synthesis of N-doped hierarchically ordered micro-mesoporous carbons for CO_2 adsorption. Journal of CO_2 Utilization, 62, 102081. doi: https://doi.org/10.1016/j.jcou.2022.102081

[14] Spessato, L., Duarte, V. A., Fonseca, J. M., Arroyo, P. A., Almeida, V. C. (2022). Nitrogen-doped activated carbons with high performances for CO_2 adsorption. Journal of CO_2 Utilization, 61, 102013. doi: https://doi.org/10.1016/j.jcou.2022.102013

[15] Mbarki, F., Selmi, T., Kesraoui, A., Seffen, M. (2022). Low-cost activated carbon preparation from Corn stigmata fibers chemically activated using H_3PO_4, $ZnCl_2$ and KOH: Study of methylene blue adsorption, stochastic isotherm and fractal kinetic. Industrial Crops and Products, 178, 114546. doi: https://doi.org/10.1016/j.indcrop.2022.114546

[16] Negara, D. N. K. P., Nindhia, T. G. T., Surata, I. W., Hidajat, F., Sucipta, M. (2020). Textural characteristics of activated carbons derived from tabah bamboo manufactured by using H_3PO_4 chemical activation. Materials Today: Proceedings, 22, 148–155. doi: https://doi.org/10.1016/j.matpr.2019.08.030

[17] Negara, D. N. K. P., Nindhia, T. G. T., Lusiana, Astika, I. M., Kencanawati, C. I. P. K. (2020). Development and Characterization of Activated Carbons Derived from Lignocellulosic Material. Materials Science Forum, 988, 80–86. doi: https://doi.org/10.4028/www.scientific.net/msf.988.80

[18] Kumar, A., Gupta, H. (2020). Activated carbon from sawdust for naphthalene removal from contaminated water. Environmental Technology & Innovation, 20, 101080. doi: https://doi.org/10.1016/j.eti.2020.101080

[19] Oladimeji, T. E., Odunoye, B. O., Elehinafe, Francis. B., Obanla, O., R., Odunlami, O., A. (2021). Production of activated carbon from sawdust and its efficiency in the treatment of sewage water. Heliyon, 7 (1), e05960. doi: https://doi.org/10.1016/j.heliyon.2021.e05960

[20] Ramirez, A., Ocampo, R., Giraldo, S., Padilla, E., Flórez, E., Acelas, N. (2020). Removal of Cr (VI) from an aqueous solution using an activated carbon obtained from teakwood sawdust: Kinetics, equilibrium, and density functional theory calculations. Journal of Environmental Chemical Engineering, 8 (2), 103702. doi: https://doi.org/10.1016/j.jece.2020.103702

[21] Canales-Flores, R. A., Prieto-García, F. (2020). Taguchi optimization for production of activated carbon from phosphoric acid impregnated agricultural waste by microwave heating for the removal of methylene blue. Diamond and Related Materials, 109, 108027. doi: https://doi.org/10.1016/j.diamond.2020.108027

[22] Li, M., Xiao, R. (2019). Preparation of a dual Pore Structure Activated Carbon from Rice Husk Char as an Adsorbent for CO_2 Capture. Fuel Processing Technology, 186, 35–39. doi: https://doi.org/10.1016/j.fuproc.2018.12.015

[23] Saberian, M., Li, J., Donnoli, A., Bonderenko, E., Oliva, P., Gill, B. et al. (2021). Recycling of spent coffee grounds in construction materials: A review. Journal of Cleaner Production, 289, 125837. doi: https://doi.org/10.1016/j.jclepro.2021.125837

[24] Mengesha, D. N., Abebe, M. W., Appiah-Ntiamoah, R., Kim, H. (2022). Ground coffee waste-derived carbon for adsorptive removal of caffeine: Effect of surface chemistry and porous structure. Science of The Total Environment, 818, 151669. doi: https://doi.org/10.1016/j.scitotenv.2021.151669

[25] Hadebe, L., Cele, Z., Gumbi, B. (2022). Properties of porous carbon electrode material derived from biomass of coffee waste grounds for capacitive deionization. Materials Today: Proceedings, 56, 2178–2183. doi: https://doi.org/10.1016/j.matpr.2021.11.496

[26] Ferraz, F. M., Yuan, Q. (2020). Organic matter removal from landfill leachate by adsorption using spent coffee grounds activated carbon. Sustainable Materials and Technologies, 23, e00141. doi: https://doi.org/10.1016/j.susmat.2019.e00141

[27] Mahanim, S. M. A., Wan Asma, I., Rafidah, J., Puad, E., Shaharuddin, H. (2011). Production of Activated Carbon from Industrial Bamboo Wastes. Journal of Tropical Forest Science, 23 (4), 417–424. Available at: https://www.researchgate.net/publication/267827623_Production_of_Activated_Carbon_from_Industrial_Bamboo_Wastes

[28] Hossain, R., Nekouei, R. K., Mansuri, I., Sahajwalla, V. (2021). In-situ O/N-heteroatom enriched activated carbon by sustainable thermal transformation of waste coffee grounds for supercapacitor material. Journal of Energy Storage, 33, 102113. doi: https://doi.org/10.1016/j.est.2020.102113

[29] Kiełbasa, K., Bayar, Ş., Varol, E. A., Sreńscek-Nazzal, J., Bosacka, M., Michalkiewicz, B. (2022). Thermochemical conversion of lignocellulosic biomass – olive pomace – into activated biocarbon for CO_2 adsorption. Industrial Crops and Products, 187, 115416. doi: https://doi.org/10.1016/j.indcrop.2022.115416

[30] Jin, C., Sun, J., Bai, S., Zhou, Z., Sun, Y., Guo, Y. et al. (2022). Sawdust wastes-derived porous carbons for CO_2 adsorption. Part 2. Insight into the CO_2 adsorption enhancement mechanism of low-doping of microalgae. Journal of Environmental Chemical Engineering, 10 (5), 108265. doi: https://doi.org/10.1016/j.jece.2022.108265

[31] Ji, Y., Zhang, C., Zhang, X. J., Xie, P. F., Wu, C., Jiang, L. (2022). A high adsorption capacity bamboo biochar for CO_2 capture for low temperature heat utilization. Separation and Purification Technology, 293, 121131. doi: https://doi.org/10.1016/j.seppur.2022.121131

[32] Xu, Y., Yang, Z., Zhang, G., Zhao, P. (2020). Excellent CO_2 adsorption performance of nitrogen-doped waste biocarbon prepared with different activators. Journal of Cleaner Production, 264, 121645. doi: https://doi.org/10.1016/j.jclepro.2020.121645

[33] Singh, J., Basu, S., Bhunia, H. (2019). Dynamic CO_2 adsorption on activated carbon adsorbents synthesized from polyacrylonitrile (PAN): Kinetic and isotherm studies. Microporous and Mesoporous Materials, 280, 357–366. doi: https://doi.org/10.1016/j.micromeso.2019.02.031

[34] Lu, T., Bai, J., Demir, M., Hu, X., Huang, J., Wang, L. (2022). Synthesis of potassium Bitartrate-derived porous carbon via a facile and Self-Activating strategy for CO_2 adsorption application. Separation and Purification Technology, 296, 121368. doi: https://doi.org/10.1016/j.seppur.2022.121368

[35] Li, J., Bao, A., Chen, J., Bao, Y. (2022). A green route to CO_2 adsorption on biomass chitosan derived nitrogen-doped micropore-dominated carbon nanosheets by different activators. Journal of Environmental Chemical Engineering, 10 (1), 107021. doi: https://doi.org/10.1016/j.jece.2021.107021

[36] Surra, E., Ribeiro, R. P. P. L., Santos, T., Bernardo, M., Mota, J. P. B., Lapa, N., Esteves, I. A. A. C. (2022). Evaluation of activated carbons produced from Maize Cob Waste for adsorption-based CO_2 separation and biogas upgrading. Journal of Environmental Chemical Engineering, 10 (1), 107065. doi: https://doi.org/10.1016/j.jece.2021.107065

[37] Serafin, J., Sreńscek-Nazzal, J., Kamińska, A., Paszkiewicz, O., Michalkiewicz, B. (2022). Management of surgical mask waste to activated carbons for CO_2 capture. Journal of CO_2 Utilization, 59, 101970. doi: https://doi.org/10.1016/j.jcou.2022.101970

Received date 30.11.2022
Accepted date 28.02.2023
Published date 22.03.2023

How to cite: *Putra Negara, D. N. K., Widiyarta, I. M., Suriadi, I. G. A. K., Dwijana, I. G. K., Budiana Penindra, I. M. D., Tenaya, I. G. N. P., Sukadana, I. G. K., Ferdinand, A. S. (2023). Development of mesoporous activated carbons derived from brewed coffee waste for CO_2 adsorption. EUREKA: Physics and Engineering, 2, 17–27. doi: https://doi.org/10.21303/2461-4262.2023.002809*